Nonvolatile resistive switching memory utilizing gold nanocrystals embedded in zirconium oxide

Weihua Guan, Shibing Long, Rui Jia, and Ming Liu[a)]
Laboratory of Nano-Fabrication and Novel Devices Integrated Technology, Institute of Microelectronics, Chinese Academy of Sciences, Beijing 100029, Republic of China

(Received 12 May 2007; accepted 26 June 2007; published online 9 August 2007)

Resistive switching characteristics of ZrO_2 films containing gold nanocrystals (nc-Au) are investigated for nonvolatile memory applications. The sandwiched top electrode/ZrO_2 (with nc-Au embedded)/n^+ Si structure exhibits two stable resistance states (high-resistance state and low-resistance state). By applying proper voltage bias, resistive switching from one state to the other state can be achieved. This resistive switching behavior is reproducible and the ratio between the high and low resistances can be as high as two orders. The intentionally introduced nc-Au in ZrO_2 films can improve the device yield greatly. ZrO_2 films with gold nanocrystals embedded are promising to be used in the nonvolatile resistive switching memory devices. © *2007 American Institute of Physics*. [DOI: 10.1063/1.2760156]

With conventional flash memories approaching their scaling limit, a great amount of research efforts have focused their attention on the next generation memory devices. Recently, reversible and reproducible resistive switching phenomena induced by applied electric field have been extensively studied due to its potential applications in resistive random access memories (RRAM).[1–6] The candidate materials for this type of memories include ferromagnetic material such as $Pr_{1-x}Ca_xMnO_3$,[1] doped perovskite oxide such as $SrZrO_3$ (Ref. 2) and $SrTiO_3$,[3] organic materials such as poly (*N*-vinylcarbazole),[4] and binary transition metal oxides.[5–7] For organic materials, several research groups have recently demonstrated resistive switching behavior for the organic bistable devices with organic/nanocrystal/organic structure sandwiched between two metal electrodes.[8–10] However, the organic material is not thermally stable and compatible with the current complementary metal oxide semiconductor technology. This is not the case for binary transition metal oxide such as NiO,[5] TiO_2,[6] and Cu_xO.[7] Compared with the other complex composition materials, they have the advantages of simple structure and easy fabrication process. Lee *et al.* have recently reported the resistive switching behavior of nonstoichiometric zirconium oxide (ZrO_x).[11] Wu *et al.* further presented a possible way to improve the device yield by replacing nonstoichiometric ZrO_x with stoichiometric ZrO_2.[12]

In this letter, we report a resistive switching memory device utilizing gold nanocrystals embedded in the zirconium oxide layer. The top metal electrode/ZrO_2 layer with gold nanocrystals embedded/n^+ Si memory cell is fabricated and investigated for the nonvolatile memory application.

The resistive switching memory devices in this study are fabricated as follows. After chemically cleaning the n^+ silicon wafer, three sequential layers of ZrO_2/Au/ZrO_2 (with thickness of 25/2/25 nm, respectively) are deposited on the substrate via e-beam evaporation. Postdeposition annealing process under several temperatures (700, 800, and 900 °C) is carried out in N_2 ambient (3 l/min) for 2 min in order to crystallize ZrO_2, passivate the defects in the film, and induce the formation of gold nanocrystals (nc-Au). Finally, 50 nm thick square-shaped Au top electrodes are evaporated and defined by the lift-off process. To confirm the role of nc-Au in resistive switching phenomenon, control samples without nc-Au in ZrO_2 matrix are simultaneously fabricated with the same process. The current-voltage (*I-V*) characteristics of the fabricated cell are analyzed by Keithley 4200 semiconductor characterization system at room temperature.

Figure 1(a) shows the cross section transmission electron microscopy (TEM) image of the microstructure for the

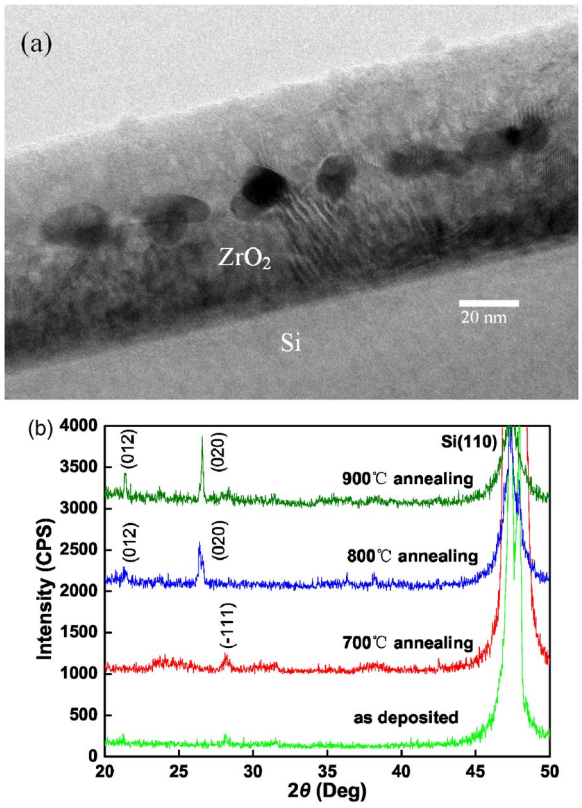

FIG. 1. (Color online) (a) Cross section TEM image of the microstructure for the sample with gold nanocrystals embedded in ZrO_2 matrix and (b) XRD patterns of ZrO_2 films annealed under various temperature conditions.

[a)]Author to whom correspondence should be addressed; FAX: 86-10-62055666; electronic mail: liuming@ime.ac.cn

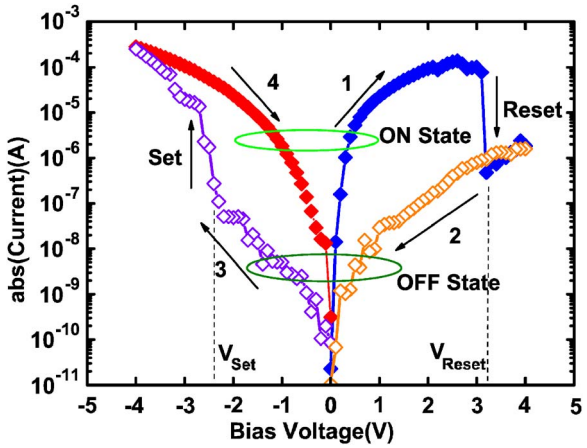

FIG. 2. (Color online) Typical *I-V* characteristics of sample Au-800 in semilog scale. The voltage is swept in the direction as follows: 0 V→4 V→0 V→−4 V→0 V.

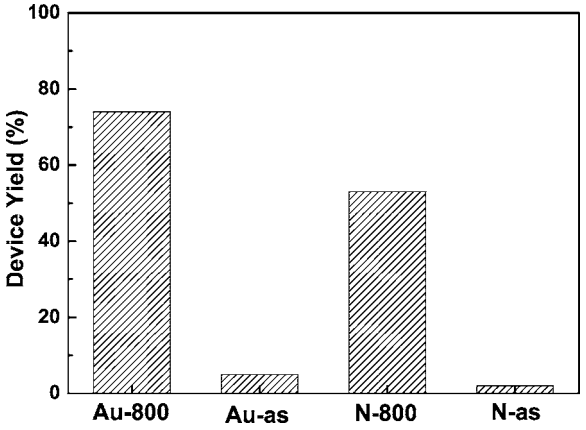

FIG. 3. Device yield comparison for four types of samples to clarify the role of nc-Au and annealing process.

sample with Au layer embedded and annealed at 800 °C. The gold nanocrystals can be clearly seen to be embedded in the ZrO_2 matrix. Figure 1(b) shows the x-ray diffraction (XRD) patterns of ZrO_2 film (without Au layer) deposited by e-beam evaporation annealed at different temperatures. As is shown that, for the as-deposited films, there are no obvious diffraction peaks, indicating an amorphous structure. ZrO_2 film after postdeposition annealing is polycrystalline. For the samples with 2 nm Au layer embedded, the same trend of x-ray diffraction patterns as Fig. 1(b) is observed.

The resistive switching behavior and memory effect of the structure are observed in the current versus voltage (*I-V*) curves. Four types of samples are electrically investigated: samples with Au layer and annealed at 800 °C (denoted as sample Au-800), samples with Au layer and as-deposited (sample Au-as), samples without Au layer and annealed at 800 °C (sample N-800), and samples without Au layer and as-deposited (sample N-as). Figure 2 depicts the typical *I-V* curves of sample Au-800. As can be seen, a conspicuous *I-V* hysteresis is observed when the bias is swept back and forth. Resistive switching from the low-resistance state (LRS or on state) to the high-resistance state (HRS or off state) is induced in voltage sweep mode by increasing the voltage up to a value (which we here define as V_{reset}) where a sudden decrease in current *I* is observed. The current of the off state increases with increasing the voltage bias in the negative direction, and a rapid switching from off state to on state can be achieved at a negative bias voltage (which we define as V_{set}). At a proper reading voltage (e.g., 0.5 V), the resistance ratio between the two states (HRS/LRS) is nearly two orders. Thus enough margins for sensing the different resistance states are confirmed.

In order to clarify the influence of nc-Au and annealing process on the resistive switching behavior, *I-V* characteristics of the control samples (samples N-800, Au-as, and N-as) are also investigated. It is found that the as-deposited samples (samples Au-as and N-as) exhibit poor or nearly no resistive switching behavior. For the annealed samples (samples Au-800 and N-800), reproducible bipolar resistive switching phenomena are observed in most of the cells. The resistive switching behavior is independent of the existence nc-Au. Indeed, several groups have already reported resistive switching behavior of ZrO_2 without heterogeneous materials.[11–13] Au nanocrystals manifest their effect in the device yield. Figure 3 shows the device yield (percentage of the working cells) for four types of samples. It is recently reported that doped metal oxides show better device yields.[14] As a matter of fact, our samples with nc-Au embedded are somewhat comparable to the doping process in metal oxides.

By far, although a variety of transition metal oxides have been found to have the resistive switching characteristics and several hypothetical models have been proposed to account for the resistive switching phenomena, for instance, "trap charging and discharging,"[5] and "forming and rupture of conductive filaments,"[6] the switching mechanism is still not clear yet. According to the electrical characteristics observed, we infer that the resistive switching behavior in our samples may be due to electron trapping and detrapping in nc-Au dispersed in ZrO_2, which is similar to the mechanism proposed by Lee *et al.* to explain the resistance switching behavior for Zr^+ excess nonstoichiometric ZrO2 films.[11] When electrons are injected and trapped in nc-Au by applying a positive voltage (e.g., V_{reset}), an interior electric field is built in the ZrO_2 layer, resulting in the decrease of the conductivity and thus the increase of the resistance, which corresponds to the reset process. When a negative voltage (e.g., V_{set}) is applied, electrons are ejected out of the nc-Au and as a result, the conductivity increases, corresponding to the set process.

According to the resistive switching mechanisms proposed above, it is obvious that the defects and the traps in the ZrO_2 film play an important role in resistive switching behavior. Since the ZrO_2 film is deposited rather than grown as a single crystal, it is of an imperfect nature with a large number of defects. Moreover, a variety of materials reported to possess the resistive switching characteristics are all involved with defects. For example, metallic defects,[5] oxygen vacancies,[6] dislocations,[15] and intentionally metal doping.[2,3,14,16] In general, there are mainly two kinds of defects in the functional ZrO_2 film in our case. One is the naturally formed defects such as dislocation, grain boundary, and vacancy. The other is the intentionally introduced nc-Au, acting as the electron traps. Obviously, it is not easy to exactly control the naturally formed defects. Defects in the functional ZrO_2 film vary from cell to cell and thus lead to unstable resistive switching performances. The introduction of nc-Au, which is more controllable, provides another dimension in modulating the traps in ZrO_2 film. As a result, the

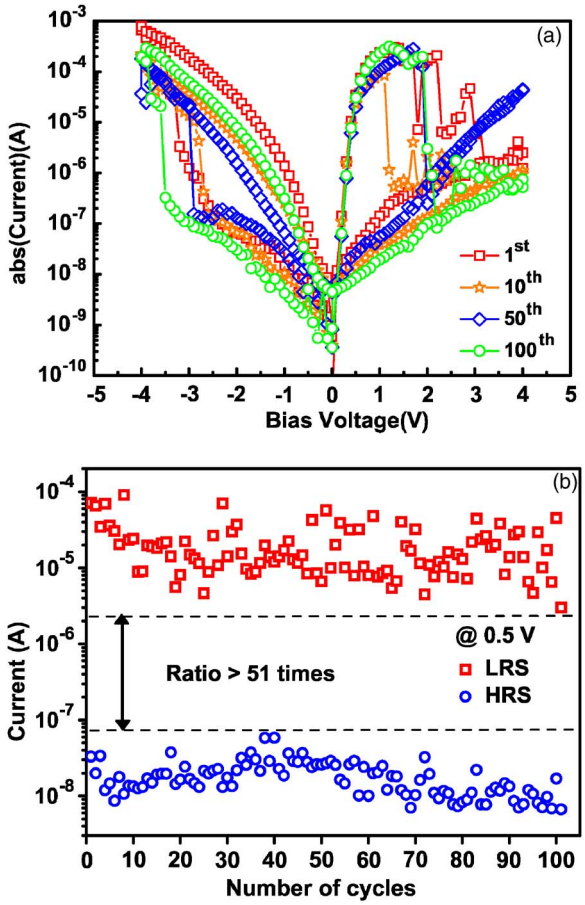

FIG. 4. (Color online) Endurance performance of the sample Au-800. More than 100 write-erase cycles is demonstrated. (a) The plot of the current vs the voltage curve for a certain times cycles which varies a little. (b) The currents of HRS and LRS vs the number of switching cycles at 0.5 V reading voltage.

device yield can be improved since trap concentrations are more uniform and homogeneous in each cell.

Figure 4(a) shows the result of cycling tests for sample Au-800. More than 100 times of set/reset cycles without sensing margin deterioration have been demonstrated. Figure 4(b) shows the current of the HRS and LRS versus the number of switching cycles at 0.5 V reading voltage. As is shown, at least 50 times ratio between HRS and LRS can be guaranteed, large enough for the periphery circuits to probe the different resistance states. The nonvolatile characteristics of the fabricated memory devices are also investigated. Figure 5 shows the variation of the resistance with time at both the HRS and LRS for sample Au-800. As can be seen, the variation of LRS and HRS resistance after 1000 seconds is found to be very little, confirming the nonvolatile nature of the device.

In summary, the top electrode/ZrO_2 with nc-Au embedded/n^+ Si sandwich structure is fabricated for the nonvolatile memory applications. The intentionally introduced nc-Au, acting as the electron traps, provides an effective way to improve the device yield. The fabricated devices possess the properties of reversible and reproducible resistance switching, nondestructive readout, good cycling performance, and nonvolatility. As a result, high potentiality of ZrO_2 films with nc-Au embedded for the nonvolatile resistive switching memory applications is confirmed.

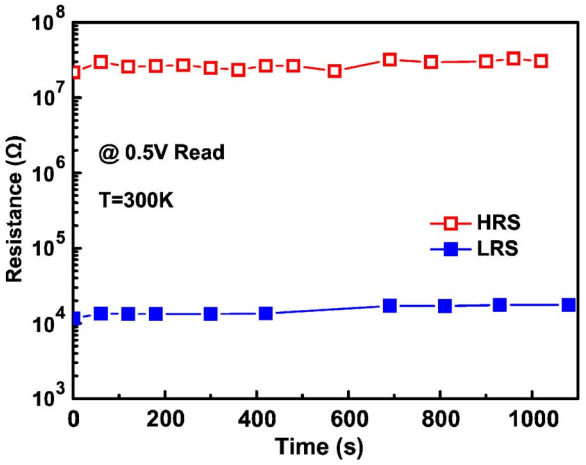

FIG. 5. (Color online) Stability of cell resistance at room temperature in both the LRS and HRS.

The authors would like to thank J. Wang (Xi'an Jiao Tong University) for XRD analysis and L. Zhen for sample preparation. This work is partly supported by National Basic Research Program of China (973 Program) under Grant No. 2006CB302706 and National Natural Science Foundation of China under Grant Nos. 90607022, 90401002, and 60506005.

[1]S. Q. Liu, N. J. Wu, and A. Ignatiev, Appl. Phys. Lett. **76**, 2749 (2000).
[2]A. Beck, J. G. Bednorz, Ch. Gerber, C. Rossel, and D. Widmer, Appl. Phys. Lett. **77**, 139 (2000).
[3]Y. Watanabe, J. G. Bednorz, A. Bietsch, Ch. Gerber, D. Widmer, A. Beck, and S. J. Wind, Appl. Phys. Lett. **78**, 3738 (2001).
[4]Y.-S. Lai, C.-H. Tu, D.-L. Kwong, and J. S. Chen, Appl. Phys. Lett. **87**, 122101 (2005).
[5]S. Seo, M. J. Lee, D. H. Seo, E. J. Jeoung, D.-S. Suh, Y. S. Joung, I. K. Yoo, I. R. Hwang, S. H. Kim, I. S. Byun, J.-S. Kim, J. S. Choi, and B. H. Park, Appl. Phys. Lett. **85**, 5655 (2004).
[6]B. J. Choi, D. S. Jeong, S. K. Kim, S. Choi, J. H. Oh, C. Rohde, H. J. Kim, C. S. Hwang, K. Szot, R. Waser, B. Reichenberg, and S. Tiedke, J. Appl. Phys. **98**, 033715 (2005).
[7]R. Dong, D. S. Lee, W. F. Xiang, S. J. Oh, D. J. Seong, S. H. Heo, H. J. Choi, M. J. Kwon, S. N. Seo, M. B. Pyun, M. Hasan, and H. Hwang, Appl. Phys. Lett. **90**, 042107 (2007).
[8]L. P. Ma, J. Liu, and Y. Yang, Appl. Phys. Lett. **80**, 2997 (2002).
[9]J. H. Jung, J.-H. Kim, T. W. Kim, M. S. Song, Y.-H. Kim, and S. Jin, Appl. Phys. Lett. **89**, 122110 (2006).
[10]Y. Song, Q. D. Ling, S. L. Lim, E. Y. H. Teo, Y. P. Tan, L. Li, E. T. Kang, D. S. H. Chan, and C. Zhu, IEEE Electron Device Lett. **28**, 107 (2007).
[11]D. S. Lee, H. J. Choi, H. J. Sim, D. H. Choi, H. S. Hwang, M.-J. Lee, S.-A. Seo, and I. K. Yoo, IEEE Electron Device Lett. **26**, 719 (2005).
[12]X. Wu, P. Zhou, J. Li, L. Y. Chen, H. B. Lv, Y. Y. Lin, and T. A. Tang, Appl. Phys. Lett. **90**, 183507 (2007).
[13]C.-Y. Lin, C.-Y. Wu, C.-Y. Wu, T.-C. Lee, F.-L. Yang, C. Hu, and T.-Y. Tseng, IEEE Electron Device Lett. **28**, 366 (2007).
[14]D. S. Lee, D. J. Seong, H. J. Choi, I. Jo, R. Dong, W. Xiang, S. K. Oh, M. B. Pyun, S. O. Seo, S. H. Heo, M. S. Jo, D. K. Hwang, H. K. Park, M. Chang, M. Hasan, and H. S. Hwang, Tech. Dig. - Int. Electron Devices Meet. **2006**, 439.
[15]K. Szot, W. Speier, G. Bihlmayer, and R. Waser, Nat. Mater. **5**, 312 (2006).
[16]D. Lee, D. Seong, I. Jo, F. Xiang, R. Dong, S. Oh, and H. Hwang, Appl. Phys. Lett. **90**, 122104 (2007).